Journal of Alloys and Compounds 503 (2010) 345–349

Contents lists available at ScienceDirect

Journal of Alloys and Compounds

journal homepage: www.elsevier.com/locate/jallcom

Improved dehydrogenation performance of $LiBH_4/MgH_2$ composite with Pd nanoparticles addition

B.C. Weng[a,*], X.B. Yu[b], Z. Wu[a,*], Z.L. Li[a], T.S. Huang[a], N.X. Xu[a], J. Ni[a]

[a] Shanghai Institute of Microsystem and Information Technology, Chinese Academy of Sciences, Shanghai 200050, China
[b] Department of Materials Science, Fudan University, Shanghai 200433, China

ARTICLE INFO

Article history:
Received 7 July 2009
Received in revised form 15 October 2009
Accepted 8 November 2009
Available online 13 November 2009

Keywords:
Lithium borohydride
Hydrogen storage material
Magnesium hydride
Pd nanoparticles

ABSTRACT

The hydrogen storage properties of $LiBH_4/MgH_2$ ball milled with Pd nanoparticles were investigated. By introduction of Pd nanoparticles, the initial dehydrogenation temperature of the composite decreases from 340 to 260 °C and the total weight loss reaches up to 8.0 wt.% below 400 °C. Rehydrogenation results show 7.9 wt.% hydrogen can be rehydrogenated from the dehydrogenated product at 400 °C under 35 atm of hydrogen for 6 h. XRD analysis demonstrates that the hydrogen desorption of the Pd doped $LiBH_4/MgH_2$ mixture mainly includes two steps: first, at temperature above 260 °C, magnesium hydride reacts with Pd nanoparticles to generate Mg_6Pd and the decomposition of MgH_2; and then, above 350 °C, magnesium reacts with $LiBH_4$ to form MgB_2 and LiH.

1. Introduction

Hydrogen is widely considered as an ideal energy carrier because its combustion product is water, a zero pollutant. However, safe and efficient hydrogen storage as well as hazards associated with hydrogen transportation are critical challenges that must be overcome in order for hydrogen to play a key role in meeting humankind's future energy needs [1].

As solid-state hydrogen storage medium, the metal hydrides have high volumetric hydrogen capacity as compared to other storage options such as high pressure cylinders and liquid hydrogen. It has been found that hydrides offer an efficient and safe way for storing hydrogen [2]. Unfortunately, high volumetric hydrogen storage capacity in most of these hydrides is being offset by their low gravimetric hydrogen storage capacity, which is generally to be of the order of 1–2 wt.% [3]. One of the ways to overcome this difficulty is using high hydrogen content compounds such as MH_x (*e.g.* LiH or MgH_2) [4–6], amides (NH_2^-) [7], alanate (AlH_4^-) [8,9] and borohydride (BH_4^-) [10–15], which possess hydrogen gravimetric capacity >5 wt.%. Among them $LiBH_4$ has quite high theoretical gravimetric (18.5 wt.%) and volumetric (121 g L^{-1}) hydrogen storage capacities, potentially being a superior hydrogen storage material. However, the thermodynamic and kinetic limitations that are essentially imposed by the involved strong covalent and ionic bonds greatly restrain the practical applications of $LiBH_4$ [2,7,14–17].

More recently, research in this field has focused on reacting the complex hydride with another hydride (in this case a binary hydride) to form a mixed compound in the dehydrogenated state [18]. Vajo et al. [19] found that $LiBH_4$ may be reversibly dehydrogenated and rehydrogenated with a reduced reaction enthalpy by the addition of MgH_2. They believed that reaction pathway is created through the formation of MgB_2:

$$LiBH_4 + 1/2MgH_2 \rightarrow LiH + 1/2MgB_2 + 2H_2 \quad (1)$$

The formation of MgB_2 stabilizes the dehydrogenated state and effectively destabilizes $LiBH_4$.

Yu et al. [10] demonstrated that the decomposition of $LiBH_4/MgH_2$ mixture proceeds in three steps:

$$MgH_2 \rightarrow Mg + H_2 \quad (2)$$

$$LiBH_4 \rightarrow LiH + B + 2H_2 \quad (3)$$

$$Mg + 0.3LiH + 0.3B \rightarrow 0.37Li_{0.184}Mg_{0.186} + 0.15MgB_2 + 0.78Li_{0.3}Mg_{0.7} + 0.15H_2 \quad (4)$$

MgH_2 decomposes into Mg and H_2, then Mg catalyzes the dehydrogenation of $LiBH_4$ forming LiH and B. Above 420 °C, Mg expedites the dehydrogenation of LiH resulting in the formation of Li–Mg phases and MgB_2. The Li–Mg intermediate phases are unstable. Above 500 °C, it forms $Li_{0.184}Mg_{0.186}$, and at temperature higher

* Corresponding authors. Tel.: +86 21 6251 1070; fax: +86 21 3220 0534.
E-mail addresses: bcweng@mail.sim.ac.cn (B.C. Weng), wuzhu@mail.sim.ac.cn (Z. Wu).

0925-8388/$ – see front matter © 2009 Published by Elsevier B.V.
doi:10.1016/j.jallcom.2009.11.059

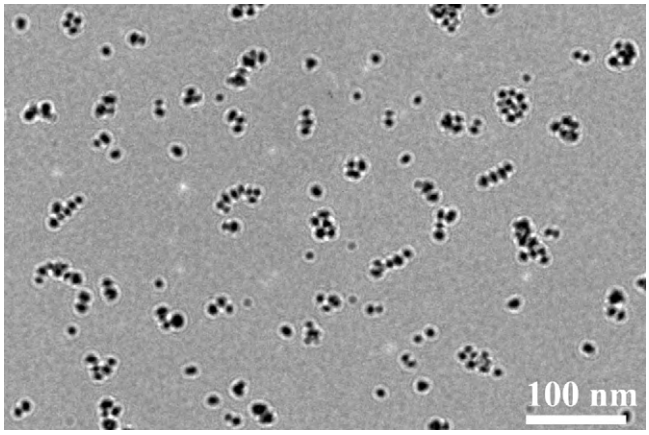

Fig. 1. TEM image of Pd nanoparticles.

than 600 °C, it forms $Li_{0.3}Mg_{0.7}$. The formation of Li–Mg alloy is prior to that of MgB_2.

Xu et al. [20] reported the catalyst effect of Pd on the dehydrogenation kinetics of $LiBH_4$. The addition of Pd showed a positive effect on dehydrogenation/rehydrogenation process of $LiBH_4$. Higuchi et al. [21] and Fischer et al. [22] investigated hydrogen storage properties of a sputtered Pd/Mg (800 nm thick)/Pd film. They found the synergetic effect in the multilayer films, in which the hydrogen desorption temperature of the Mg layer is dramatically reduced. Catalysts help the dissociation of H_2 molecules or the recombination of H atoms. Mechanisms such as the 'hydrogen pump' and the 'spillover effect' have been proposed to explain the catalytic effect. These results demonstrate the positive effect of Pd on $LiBH_4$ and Mg. However, to date, no investigations were conducted on the dehydrogenation performance of the $LiBH_4/MgH_2$ system with nano-Pd addition. In this paper, the hydrogen storage properties of $LiBH_4/MgH_2$ doped with Pd nanoparticles were investigated systemically. As expected, mechanically milling $LiBH_4/MgH_2$ composite doped with nano-Pd results in improvement of dehydrogenation kinetics. Based on the results of phase analysis, the mechanism underlying the observed performance improvement is discussed.

2. Experimental

Magnesium hydride (MgH_2) (98% purity, Alfa Aesa) and lithium borohydride ($LiBH_4$) (95% purity, Sigma–Aldrich) were used as received. PVP-protected Pd nanoparticles were prepared by ascorbic acid reduction in an oil-in-water (O/W) reverse microemulsion of water–poly(N-vinyl-2-pyrrolidone) (PVP) as detailed in Ref. [23]. Pd nanoparticles suspension was directly deposited on a carbon-coated copper grid and vacuumed dry. The morphology and size of the nanoparticles were characterized by TEM (transmission electron microscopy, JEOL 2100F, Japan). Fig. 1 shows the TEM image of the Pd nanoparticles, the nanoparticles have a narrow size distribution with an average diameter of 25 nm. The obtained nanoparticles were washed three times with excess amount of deionized water and then rinsed with ethanol and acetone in sequence, followed by drying at 70 °C under vacuum overnight. All sample handling was performed in an MBraun Labmaster 130 glovebox under argon atmosphere with <0.1 ppm O_2 and H_2O vapor. 1.6 g of MgH_2 (0.06 mol), 0.4 g $LiBH_4$ (0.018 mol) and 0.2 g nano-Pd (0.0019 mol) was loaded in a 50 mL hardened steel pot with a ball-to-powder ratio 20:1 in the argon filled glove box. Mechanically milling was carried out using a Fritsch Pulverisette 6 planetary ball mill (PBM) at 300 rpm for 1 h. The thermogravimetry (TG) measurements of $LiBH_4/MgH_2$ composite were carried out on a TG 209 F1 Iris apparatus (NETZSCH, Germany) between room temperature to 500 °C at a heating rate of 5 °C min^{-1}. Typical sample quantity was 5–10 mg, which was sufficient for getting accurate results due to the high sensitivity of the employed equipment. The weight loss percentage of the sample was calculated according to the total weight of $LiBH_4/MgH_2$ composite. Its dehydrogenation/hydrogenation kinetics were examined by a conventional Sievert type P–C–T apparatus in the pressure range of 0.1–35 atm at 280, 300, 350 and 400 °C, respectively without foregoing activation. X-ray diffraction data were obtained with a Rigaku D/max 2400 using Cu Kα radiation (Rigaku, Japan). Samples were mounted onto a 1 mm depth glass plate in the Ar-filled glove box and sealed with a polyvinylchloride membrane to avoid oxidation during the XRD measurements. ^{11}B magic-angle-spinning nuclear magnetic resonance (MAS-NMR) experiments were carried out at room temperature on a Bruker Advance 300 NMR spectrometer (Bruker, German) operating at 9.7 T on 128.3 MHz. Spectra were obtained using a two-channel custom-built probe with a 3 mm ZrO_2 rotor, and the magic-angle-spinning rate was set to 5 kHz to avoid the overlapping of spinning sidebands on other resonance lines. Three hundred scans were taken for the samples.

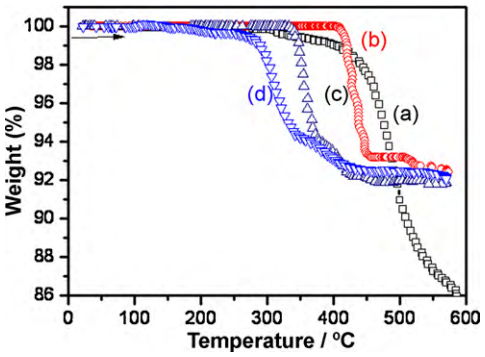

Fig. 2. TG curves for the $LiBH_4$ (a), MgH_2 (b), milled $LiBH_4/MgH_2$ mixture (c), milled $LiBH_4/MgH_2$ mixture with 10 wt.% Nano-Pd (d). All the experiments were carried out at a heating rate of 5 °C min^{-1} in argon atmosphere.

3. Results and discussion

3.1. Influence of nano-Pd on dehydrogenation properties of Li–Mg–B–H system

The TG profiles in Fig. 2 indicate the dehydrogenation behavior of $LiBH_4$, MgH_2, ball milled $LiBH_4/MgH_2$ composite and Pd nanoparticles doped composite, respectively. The onset hydrogen desorption of the ball milled $LiBH_4/MgH_2$ mixtures starts at about 340 °C, with a total weight loss of 8.0 wt.%. In the cases of nano-Pd doped $LiBH_4/MgH_2$ composite, the onset dehydrogenation temperature reduces to 260 °C. Comparable to the un-doped mixture, its total weight loss is 7.9%, indicating that addition of nano-Pd does not decrease the dehydrogenation capacity of $LiBH_4/MgH_2$ system.

It has been demonstrated that MgH_2 and $LiBH_4$ did not dehydrogenate simultaneously [10,24,25]. The first step releases H_2 via the desorption of MgH_2, whereas the second step is through the decomposition of $LiBH_4$. Fig. 3 shows the dehydrogenation curves of the composites at 280, 300, 350 and 400 °C, respectively. The nano-Pd doped composite can liberate 6.5 wt.% hydrogen below 350 °C, which slightly exceeds the theoretical hydrogen storage capacity 6.3 wt.% for MgH_2 in the mixture. It suggests that the first step of $LiBH_4/MgH_2$ mixture decomposition catalyzed by nano-Pd is completed below 350 °C. Furthermore, the second step of hydrogen release (catalyzed dehydrogenation of $LiBH_4$) starts at 350 °C, obviously lower than the corresponding initial decompo-

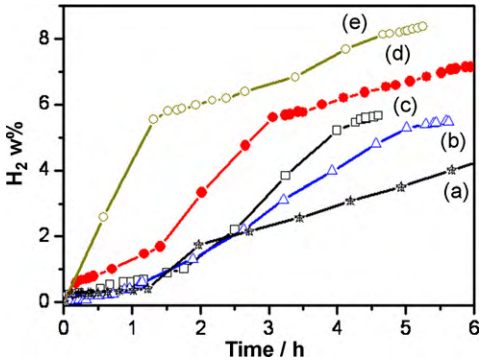

Fig. 3. Dehydrogenation curves for $LiBH_4/MgH_2$ mixture at 350 °C (a) and for nano-Pd doped $LiBH_4/MgH_2$ composite at 280 °C (b), 300 °C (c), 350 °C (d), 400 °C (e).

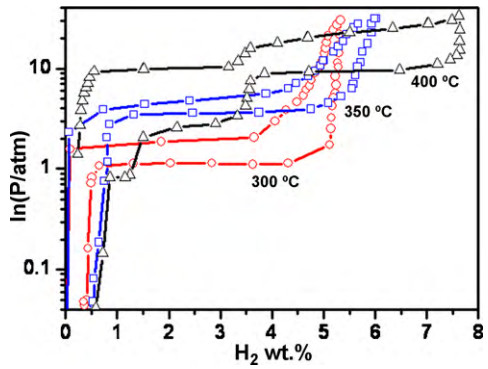

Fig. 4. PCT curves for $LiBH_4/MgH_2$ with 10 wt.% Nano-Pd at 300 °C, 350 °C, and 400 °C.

sition temperature (>420 °C) of the un-doped mixture. The above results clearly show that the dehydrogenation performance of the $LiBH_4/MgH_2$ has been significantly improved.

3.2. Influence of nano-Pd on dehydrogenation kinetics

The PCT measurement results for nano-Pd doped $LiBH_4/MgH_2$ after dehydrogenation at 300, 350 and 400 °C are shown in Fig. 4, respectively. The hydrogenation isotherms present hydrogen capacities of approximately 8 wt.% under the 35 atm H_2 at 400 °C. With temperature rising from 300 to 400 °C, the hydrogenation/dehydrogenation equilibrium pressure increases. At 300 and 350 °C, the absorption curves show a flat plateau at pressures of 1.8 and 3.7 atm, respectively. However, two flat plateaus are observed in desorption part of PCT curve at 400 °C. The difference results from the different decomposition process. The hydrogenation isotherms present reversible hydrogen capacities of approximately 6 wt.% at 350 °C and 8 wt.% at 400 °C.

3.3. Effect of Pd catalyst on composite structure

Fig. 5 shows the XRD results for the phase changes of nano-Pd doped $LiBH_4/MgH_2$ mixture during the dehydrogenation process. The d-spacings values in Fig. 5 are listed in Table 1. As Fig. 5 indicated, the XRD peaks of the as-prepared nano-Pd doped $LiBH_4/MgH_2$ correspond to MgH_2 and $PdH_{0.706}$ along with a very weak peak for $LiBH_4$ phase, suggesting that Pd forms $PdH_{0.706}$ ball

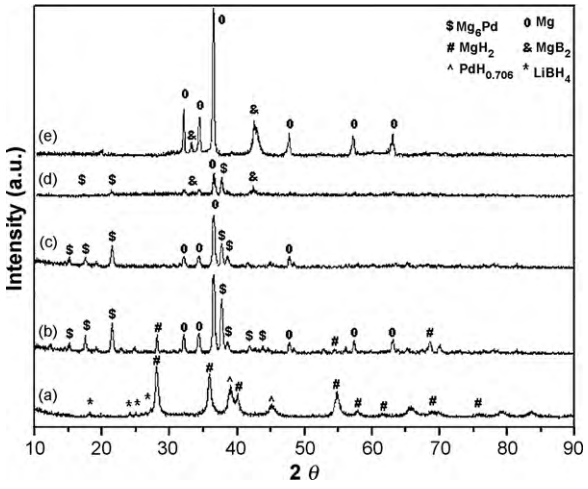

Fig. 5. XRD patterns for $LiBH_4/MgH_2$ mixture doped with nano-Pd after ball milled for 1 h (a), dehydrogenated at 280 °C (b), 350 °C (c), and 400 °C (d) and composite without Pd dehydrogenated at 600 °C (e).

milled with $LiBH_4$ and MgH_2. Because of low content of $PdH_{0.706}$ (0.0019 mol in the mixture) and the very weak peak for $LiBH_4$ phase, it is hard to identify the source of H atoms in $PdH_{0.706}$. After heating from 260 to 350 °C, the XRD patterns show metallic Mg and Mg_6Pd, whereas $PdH_{0.706}$ and $LiBH_4$ disappear, and when heating up to 350 °C, MgH_2 diffraction peaks disappear, suggesting that the first dehydrogenation step includes two hydrogen release reactions: the reaction of magnesium hydride with palladium hydride to form Mg_6Pd and the decomposition of MgH_2. The content of Pd in the composite is very low (0.0019 mol), so the hydrogen release during the first dehydrogenation step is mainly from the decomposition of MgH_2.

No pattern for the borohydride phase is detected from XRD results which might be due to its poor crystallinity after the first step. Fig. 6 shows the ^{11}B NMR spectra of the sample during the first dehydrogenation step. ^{11}B chemical shifts are referenced to solid $NaBH_4$ (−41 ppm). As shown in Fig. 6, as-prepared sample exhibits a wide resonance at −40 ppm, which is consistent with the previously published NMR data for the $LiBH_4$ specie [26]. After heating to 280 °C, the $LiBH_4$ resonance can still be clearly identified without chemical shift changes, suggesting that $LiBH_4$ is chemically inert in the composite below 280 °C. Heating the sample up to 350 °C, the ^{11}B NMR spectra shows a wide peak ($\Delta\upsilon_{1/2}$ of ~52 kHz), which is an evidence of delocalized electron cloud distribution around the boron atom leading to the anisotropic bulk magnetic susceptibility that cannot be eliminated completely by magic-angle-spinning [27]. Additionally, the simulating plot shown in Fig. 6B indicates that the peak is overlapped by several resonance peaks ranging from 100 to −80 ppm (corresponding to MgB_2, BH_4^-, BH_x species) [26]. These results clearly demonstrate that $LiBH_4$ and MgH_2 are dehydrogenated sequentially, $LiBH_4$ is chemically stable during the first dehydrogenation step and its decomposition temperature is higher than 350 °C.

The dehydrogenation process is postulated as:

$$MgH_2 \rightarrow Mg + H_2 \quad (5)$$

$$6MgH_2 + PdH_{0.706} \rightarrow Mg_6Pd + 6.353H_2 \quad (6)$$

The XRD results demonstrate that nano-Pd catalyzes the dehydrogenation of $LiBH_4/MgH_2$ mixture by reacting with Mg to form Mg_6Pd and decreasing the initial decomposition temperature.

When further heating to 400 °C, the XRD patterns consist of peaks for Mg, Mg_6Pd and MgB_2, suggesting that $LiBH_4$ is dehydrogenated at the second step. It was reported that Mg catalyzed the dehydrogenation of borohydride to form MgB_2 in $LiBH_4/MgH_2$ composite only at a higher temperature (>450 °C) [10]. However, after doping with nano-Pd, MgB_2 was formed below 400 °C. As no apparent change of Mg_6Pd phase was observed during the second dehydrogenation step, Mg_6Pd seemed to act as a catalyst. Therefore the second dehydrogenation reaction could be postulated as:

$$0.3LiBH_4 + Mg \overset{350-400^\circ C}{\longrightarrow} 0.3LiH + 0.15MgB_2 + 0.85Mg + 0.45H_2 \quad (7)$$

Based on these two dehydrogenation reaction Eqs. (6) and (7), the theoretical total hydrogen release capacity from $LiBH_4/MgH_2$ catalyzed by nano-Pd is 8.7 wt.%, and the experimental hydrogen release amount is 8.3 wt.% (shown in Fig. 3), which is close to the theoretical capacity. The above results obviously show that under the catalyst effect of nano-Pd, the hydrogen can be totally released from $LiBH_4/MgH_2$ mixtures as the following formula

$$LiBH_4 + 1/2MgH_2 \rightarrow LiH + 1/2MgB_2 + 2H_2 \quad (8)$$

To explore structural change during the rehydrogenation process, a sequence of XRD measurements is shown in Fig. 7. Rehydrogenation at 400 °C for 2 h leads to the formation of MgH_2 phase and the disappearance of MgB_2. Furthermore, after rehydrogenated at 400 °C for 6 h, the XRD patterns reveal the formation

Table 1
Comparison of d-spacings for phases observed of $LiBH_4/MgH_2$ composite in Figs. 5 and 7.

Phases	d-Spacings						References
$LiBH_4$	4.8871	3.6931	3.2805				This work
	4.9600	3.7000	3.3000				PDF#27-0287
MgH_2	3.1796	2.2522	1.6749	1.3634			This work
	3.1870	2.2570	1.6790	1.3640			PDF#35-1185
$PdH_{0.706}$	2.3198	2.0069	1.4189	1.2107			This work
	2.3200	2.0100	1.4213	1.2120			PDF#18-0951
Mg	2.7814	2.6155	2.4599	1.9050	1.6062	1.4754	This work
	2.7790	2.6051	2.4520	1.9006	1.6044	1.4728	PDF#65-3365
Mg_6Pd	5.8074	5.0750	4.6309	4.1164	2.3794	2.3285	This work
	5.8050	5.0270	4.6130	4.1050	2.3700	2.3220	PDF#25-1084
MgB_2	2.6763	2.1309					This work
	2.6741	2.1295					PDF#38-1369

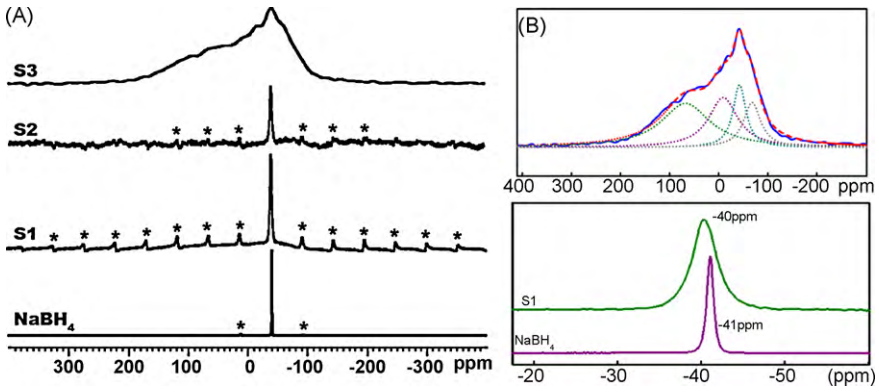

Fig. 6. (A) ^{11}B NMR spectra of $LiBH_4/MgH_2$ mixture doped with nano-Pd after ball milled for 1 h (S1), dehydrogenated at 280 °C (S2), at 350 °C (S3). (B) the simulating plot of curve S3, solid line: measured curve of $LiBH_4/MgH_2$ mixture doped with nano-Pd dehydrogenated at 350 °C; dash line: simulating results of curve S3; dot line: simulated resonance peaks composed the measured curve. $NaBH_4$ spectra as reference sample. Peaks labeled by "*" are spinning sidebands.

of MgH_2 and $PdH_{0.706}$, whereas Mg and Mg_6Pd phases disappear, suggesting that Mg, Mg_6Pd, MgB_2 and LiH react with hydrogen to form MgH_2 and PdH during the rehydrogenation process, but no pattern is detected for the borohydride phase. Supposed the rehydrogenation by-products contain $LiBH_4$, the hydrogenation process is postulated to be:

$$2LiH + MgB_2 + Mg + Mg_6Pd + 11.5H_2 \xrightarrow{400\,^\circ C,\ 35\,atm} 8MgH_2 + PdH + 2LiBH_4 \quad (9)$$

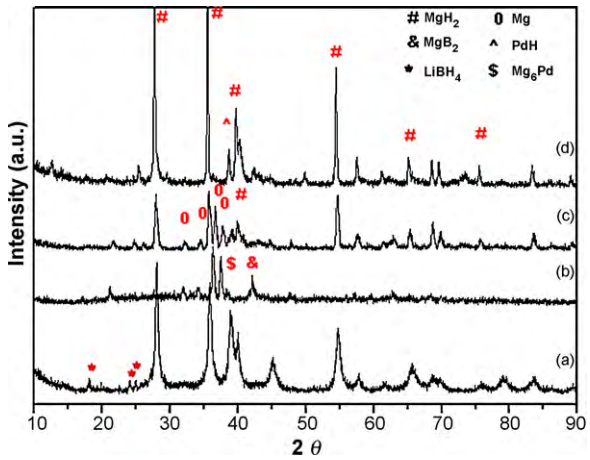

Fig. 7. XRD patterns for as milled $LiBH_4/MgH_2$ mixture doped with Pd (a), after dehydrogenated at 400 °C (b), rehydrogenated at 400 °C for 2 h (c) and rehydrogenated at 400 °C for 6 h (d).

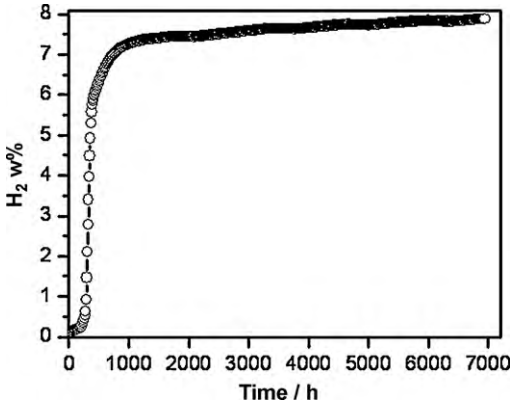

Fig. 8. The dehydrogenation curve of the sample after rehydrogenation at 400 °C for 6 h.

Based on the equation, a newly rehydrogenated mixture might reversibly store about 8.7 wt.% hydrogen at 400 °C. Both the dehydrogenation curve of the rehydrogenated $LiBH_4/MgH_2/Pd$ sample (shown in Fig. 8) and the P–C–T plot (shown in Fig. 4) show a rehydrogenation mount of 7.9 wt.%, close to the theoretical value.

4. Conclusions

Pd nanoparticles, as catalyst, play a crucial role in improving dehydrogenation of $LiBH_4/MgH_2$ mixture. The dehydrogenation behavior of $LiBH_4/MgH_2$ can be significantly improved even with

a small amount of addition. Pd nanoparticles reduce the dehydrogenation temperature of MgH_2 from 350 to 260 °C. Under the effect of nano-Pd, hydrogen in $LiBH_4/MgH_2$ can be totally released following the formula (10) under 400 °C

$$LiBH_4 + 1/2MgH_2 \rightarrow LiH + 1/2MgB_2 + 2H_2 \quad (10)$$

Furthermore, the Pd doped $LiBH_4/MgH_2$ may be reversibly dehydrogenated and rehydrogenated below 400 °C. Rehydrogenation results show 7.9 wt.% hydrogen can be rehydrogenated from the dehydrogenated product at 400 °C under 35 atm of hydrogen for 6 h. The amount of hydrogen rehydrogenated at 400 °C is close to the theoretical hydrogen capacity of 8.7 wt.% of $LiBH_4/MgH_2$ mixture. It is noteworthy that although Pd is expensive, it can be readily recycled in practical applications through hydrolyzation reaction, and our results may open a new and promising way for the nanocatalytic dehydrogenation of $LiBH_4/MgH_2$.

Acknowledgments

This work was financially supported by National "863" High-Tech. Research Programs of China (07586B1001, 07586C1002) and the SIMIT-QN Innovation Foundation (no. 119900QN04).

References

[1] Z.T. Xiong, C.K. Yong, P. Chen, W. Shaw, A. Karkamkar, Nat. Mater. 7 (2007) 138–141.
[2] L. Schlapbach, A. Züttel, Nature 414 (2001) 353–355.
[3] R.L. Cohen, J.H. Wernick, Science 214 (1981) 1081–1087.
[4] J. Vajo, F. Mertens, C.C. Ahn, R.C. Bowman, B. Fultz, J. Phys. Chem. B 108 (2004) 13977–13983.
[5] M.A. Lillo-Ródenas, K.F. Aguey-Zinsou, D. Cazorla-Amorós, J. Phys. Chem. C 112 (2008) 5984–5993.
[6] A. Léon, O. Zabara, S. Sartori, N. Eigen, M. Dornheim, T. Klassen, J. Muller, B. Hauback, M. Fichtner, J. Alloys Compd. 476 (2009) 425–428.
[7] P. Chen, Z.T. Xiong, J. Luo, J.Y. Lin, K.L. Tan, Nature 420 (2002) 302–304.
[8] Z. Lodziana, A. Züttel, J. Alloys Compd. 471 (2009) L29–L31.
[9] Z. Ma, M.Y. Zhou, J. Alloys Compd. 479 (2009) 678–683.
[10] X.B. Yu, D.M. Grant, G.S. Walker, Chem. Commun. (2006) 3906–3908.
[11] X.B. Yu, Z. Wu, Q.R. Chen, Z.L. Li, B.C. Weng, T.S. Huang, Appl. Phys. Lett. 90 (2007) 034106.
[12] J.F. Mao, Z. Wu, T.J. Chen, B.C. Weng, N.X. Xu, T.S. Huang, Z.P. Guo, H.K. Liu, D.M. Grant, G.S. Walker, X.B. Yu, J. Phys. Chem. C 111 (2007) 12495–12498.
[13] A. Züttel, P. Wenger, S. Rentsch, P. Sudan, P.H. Mauron, C.H. Emmenegger, J. Power Source 118 (2003) 1–7.
[14] S. Orimo, Y. Nakamori, A. Züttel, Mater. Sci. Eng. B 108 (2004) 51–53.
[15] G.J. Lewis, J.A. Sachtler, J.J. Low, D.A. Lesch, S.A. Faheem, P.M. Dosek, L.M. Knight, L. Halloran, C.M. Jensen, J. Yang, A. Sudik, D.J. Siegel, C. Wolverton, V. Ozolins, S. Zhang, J. Alloys Compd. 446–447 (2007) 355–359.
[16] Y.F. Liu, K. Luo, Y.F. Zhou, M.X. Gao, H.G. Pan, J. Alloys Compd. 481 (2007) 473–479.
[17] L. Mosegaard, B. Møller, J. Jørgensen, U. Bösenberg, M. Dornheim, J.C. Hanson, Y. Cerenius, G.S. Walker, H.J. Jakobsen, F. Besenbacher, T.R. Jensen, J. Alloys Compd. 446–447 (2007) 301–305.
[18] J. Yang, A. Sudik, D.J. Siegel, Angew. Chem. Int. Ed. 47 (2008) 882–887.
[19] J.J. Vajo, S.L. Skeith, F. Mertens, J. Phys. Chem. B 109 (2005) 3719–3722.
[20] J. Xu, X.B. Yu, Z.Q. Zou, Z.L. Li, Z. Wu, D.L. Akins, H. Yang, Chem. Commun. (2008) 5740–5742.
[21] K. Higuchi, K. Yamamoto, H. Kajioka, K. Toiyama, M. Honda, S. Orimo, H. Fujii, J. Alloys Compd. 330–332 (2002) 526–530.
[22] A. Fischer, A. Krozer, L. Schlapbach, Surf. Sci. 269–270 (1992) 737–742.
[23] T. Teranishi, M. Miyake, Chem. Mater. 10 (1998) 594–600.
[24] P.J. Wang, Z.Z. Fang, L.P. Ma, X.D. Kang, P. Wang, Int. J. Hydrogen Energy 33 (2008) 5611–5616.
[25] M.Q. Fan, L.X. Sun, Y. Zhang, F. Xu, J. Zhang, H.L. Chu, Int. J. Hydrogen Energy 33 (2008) 74–80.
[26] X.D. Kang, L.P. Ma, Z.Z. Fang, L.L. Gao, J.H. Luo, S.C. Wang, P. Wang, Phys. Chem. Chem. Phys. 11 (2009) 2507–2513.
[27] F.E. Pinkerton, M.S. Meyer, G.P. Meisner, M.P. Balogh, J.J. Vajo, J. Phys. Chem. C 111 (2007) 12881–12885.